PNAS RESEARCH ARTICLE | SUSTAINABILITY SCIENCE

Climate-driven divergence in biophysical and economic impacts of agrivoltaics

Mengqi Jia[a,1], Bin Peng[a,b,c,1], Kaiyu Guan[a,c,d,1], David M. Lawrence[e], Evan H. DeLucia[a,f], Alan K. Knapp[g], Greg A. Barron-Gafford[h], Madhu Khanna[a,i], Danica L. Lombardozzi[e,j], Matthew A. Sturchio[g], Steven A. Kannenberg[k], Lei Zhao[l], James McCall[m], Jinyun Tang[n], Carl J. Bernacchi[a,b,o], Paul Mwebaze[a], Fahd Majeed[a], DoKyoung Lee[a,b], and Alson Time[a]

Affiliations are included on p. 11.

Edited by B. Turner II, Arizona State University, Tempe, AZ; received June 6, 2025; accepted January 26, 2026

Increasing global demands for food and energy necessitate innovative land-use solutions. Agrivoltaics, colocating solar photovoltaics with agriculture, shows promise, but its widespread adoption faces complex biophysical and economic trade-offs in a changing climate. Here, we develop an integrated biophysical–economic modeling framework to quantify how agrivoltaics affect biophysical and economic impacts across the Midwestern United States under both current and project climate conditions. We find strong regional divergences driven by climate gradients. In the humid eastern Midwest, solar panel shading limits photosynthesis, leading to reduced yields (maize −24%; soybean −16%) and lower farmers' profitability (maize −16%; soybean −2%) compared to conventional agriculture. Conversely, in the semiarid western region, shading alleviates heat and water stress, moderating yield reductions for maize (−12%) and even boosting soybean yields (+6%), resulting in improved economic returns (−6% for maize; +9% for soybean), for a scenario with 33% photovoltaic ground coverage ratio. Although agrivoltaics generate substantial electrical energy across all regions, high upfront installation costs challenge solar developers compared to standalone solar photovoltaics. However, our analysis identifies "win-win" opportunities where soybean-based agrivoltaics in the semiarid region produce economic benefits for both farmers and solar developers, highlighting the necessity for region-specific designs tailored to local climate conditions. Critically, future climate projections indicate eastward expansion of semiarid conditions, broadening areas where agrivoltaics can mitigate crop yield penalties (even boosting yield) and improve overall profitability, especially under high-emission scenarios. The results provide a mechanistic and economically integrated understanding essential for developing evidence-based and region-specific strategies to scale agrivoltaics in a changing climate.

agrivoltaics | climates | divergent impacts | biophysical feedbacks | economic incentives

Significance

Agrivoltaics, colocating agriculture and solar photovoltaics, reduce land competition but face adoption challenges due to biophysical–economic complexities. By developing an integrated biophysical–economic modeling framework, we find significant climate-driven divergences in the US Midwest: agrivoltaics reduce crop yields and profits in the humid east but can enhance crop productivity and economic returns in the semiarid west by alleviating water stress. Despite consistent electrical energy benefits, high upfront costs challenge adoption. However, we identify promising "win-win" opportunities in semiarid soybean systems where both farmers and developers benefit. Climate projections show semiarid conditions expanding eastward by 2100, potentially broadening viable regions where agricultural and economic benefits align. This work highlights the importance of evidence-based, region-specific agrivoltaic strategies to ensure food and energy security.

Meeting the dual challenges of feeding a growing population and accelerating the clean energy transition presents one of the most pressing sustainability issues of the 21st century (1, 2). Climate change compounds this dilemma, threatening crop yields through extreme weather events while urgently necessitating the widespread deployment of renewable energy infrastructure (3, 4). Harvesting solar energy with ground-mounted photovoltaic arrays has emerged as a cost-effective strategy for meeting rising energy demand, enabling electricity generation across different landscapes while maintaining low life-cycle carbon emissions (5). With the global growth of solar energy adoption, utility-scale photovoltaics are becoming significant competitors for land. For example, solar arrays generating energy equivalent to a conventional 1 giga-watt power station (e.g., coal, natural gas, or nuclear) typically require approximately 80 km^2 of land (6). This significant land requirement raises concerns as stakeholders must make difficult decisions about land-use priorities between agriculture and energy. Agrivoltaics (Fig. 1), also termed "dual-use" photovoltaics, presents an innovative solution to this complex land-use dilemma (7–9). Integrating solar energy and agriculture on shared land offers a promising pathway to harmonize food and energy production. Such efforts may challenge the traditional view that farming and renewable energy must compete for land in a "zero-sum-game" (10, 11). Pioneering installations across the United States, European Union, and East Asia demonstrate the technology's scalability and potential to transform land productivity (12–14).

Despite potentially promising cobenefits, emerging research highlights complexities that hinder the widespread adoption of agrivoltaics in a changing climate (15, 16). Existing work focuses on isolated components of the food–energy–water nexus (17) or relies on site-specific experiments and modeling (18, 19), limiting our understanding of how integrated systems respond to deployment and environmental change. This narrow scope

The authors declare no competing interest.

This article is a PNAS Direct Submission.

[1]To whom correspondence may be addressed. Email: mengqij@illinois.edu, binpeng@illinois.edu, or kaiyug@illinois.edu.

This article contains supporting information online at https://www.pnas.org/lookup/suppl/doi:10.1073/pnas.2514380123/-/DCSupplemental.

Published March 2, 2026.

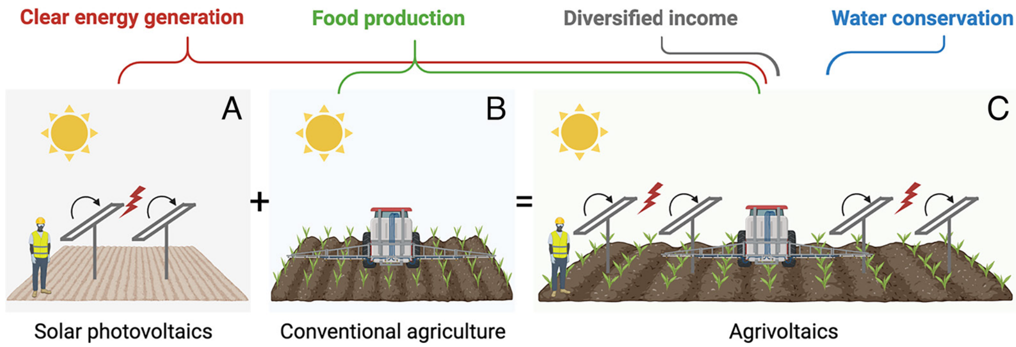

Fig. 1. Conceptual diagram of agrivoltaics colocating solar photovoltaics and conventional agriculture on the same land. (*A*) Solar panels installed by developers generate electricity; (*B*) Conventional agriculture supports food production; and (*C*) Agrivoltaics follow traditional utility-scale solar layouts, modified to allow light penetration and accommodate crop growth, harvesting equipment, and farmer access beneath and between panel rows.

hampers assessment of agrivoltaics' effects on key ecosystem functions, including land productivity (20), carbon sequestration (21), physical climate feedback (22, 23), water dynamics (24), and biodiversity (25, 26), particularly across diverse geographic and climatic gradients. Moreover, generalizing results remains difficult, as the performance and economic viability of specific agrivoltaic designs vary widely with local environmental conditions (27, 28). While advances in photovoltaic technologies and smart land management have been explored at small scales, these efforts fall short of the broader assessments. As a result, critical knowledge gaps persist in understanding how agrivoltaics can maintain ecosystem sustainability and economic resilience while adapting to climate change.

Here, we develop an integrated biophysical–economic modeling framework (*Materials and Methods*) to quantify the potential impacts of agrivoltaics on rainfed maize and soybean systems across in the Midwestern United States under current and future climate conditions. This region serves as both the nation's breadbasket and an emerging center for renewable energy development (29). The biophysical component explicitly represents agrivoltaics, enabling detailed simulation of hydrological dynamics, energy generation patterns, along with plant-soil dynamics across diverse climate conditions and system designs. This integrated capability then supports a benefit–cost analysis that examines profitability determinants for both agricultural producers and solar developers. Finally, we perform paired simulations under three distinct shared socioeconomic pathways (SSPs), including a low-emission scenario (SSP1-2.6), a high-emission scenario (SSP3-7.0), and a highest-emission scenario (SSP5-8.5), to evaluate how different development trajectories influence ecosystem sustainability and economic viability. This study provides critical insights to support evidence-based land-use planning and offer policymakers, land managers, and investors with actionable strategies for scaling agrivoltaics in regionally tailored and climate-resilient ways.

Results

Divergent Biophysical Feedbacks of Agrivoltaics. We compare multiyear (2000–2014) averaged crop yield, water-use efficiency (WUE), and land equivalent ratio (LER) between agrivoltaics (with a 33% photovoltaic ground coverage ratio (PV GCR)) and conventional agriculture (Fig. 2 *A–I* and *SI Appendix*, Figs. S1–S2). First, our analysis reveals regional differences in how agrivoltaics affect crop yields compared to conventional agriculture. In the semiarid region (i.e., most of North Dakota, South Dakota, Kansas, and western Nebraska), agrivoltaics lead to a 21.41 ± 10.96 Bu/acre (mean ± SD; the SD reflects interannual variability) (−12%) decline in maize yield but a 2.0 ± 0.7 Bu/acre (+6%) increase in soybean yield. Conversely, in both semihumid and humid regions (the other eight states), agrivoltaics decrease yields for both crops. Maize yield decreases by 26 ± 10 Bu/acre (−22%) in semihumid and 32 ± 6 Bu/acre (−24%) in humid regions, while soybean yield decreases by 4 ± 3 Bu/acre (−11%) and 6 ± 1 Bu/acre (−16%), respectively. Second, agrivoltaics consistently increase WUE across all regions compared to conventional agriculture. The largest increases are observed in the semiarid region, where maize WUE rises by 0.36 ± 0.17 gC/kg H_2O (+14%) and soybean WUE by 0.41 ± 0.13 gC/kg H_2O (+16%). Third, agrivoltaics also enhance LER (*SI Appendix, Supplementary Text: Land Equivalent Ratio Definition*) across all regions. The semiarid region demonstrates the greatest improvements, with LER for maize increasing by 0.12 ± 0.09 (+12%) and for soybean by 0.29 ± 0.14 (+29%). Building on the observed shifts in crop yields, WUE, and LER across the climate gradient, we apply linear regression to quantify how microclimatic and crop growth variables vary with the aridity index under present-day conditions. In the Midwest, solar panels consistently reduce photosynthetically active radiation (PAR), canopy temperature (CT), evapotranspiration (ET), canopy vapor-pressure deficit (CVPD), while increasing soil moisture (SM) (*SI Appendix*, Fig. S3). Regression analyses reveal that these effects vary systematically along the aridity gradient: reductions in PAR, CT, and CVPD strengthen toward more humid conditions (higher aridity index), whereas the reductions in ET and gains in SM become more pronounced toward drier regions (lower aridity index). Consequently, solar panels generally suppress gross primary productivity (GPP), plant respiration, and net primary productivity (NPP) across the humid region. However, under more arid conditions (lower aridity index), these negative crop growth responses weaken and can even reverse, indicating microclimatic buffering by panels enhances plant performance.

Beyond these climate-dependent biophysical effects, we quantify the electricity generation potential of agrivoltaics across the Midwest, assuming a 33% PV GCR. The multiyear average electrical energy flux density across the region is 41.10 ± 2.35 W/m^2 (Fig. 2*J*). This density varies with latitude, consistent with solar radiation patterns (*SI Appendix*, Fig. S4). For instance, it is highest in lower-latitude areas such as Kansas (45.56 ± 1.65 W/m^2), where the potential is greater than in higher-latitude areas like Wisconsin (38.87 ± 0.68 W/m^2). In addition, the multiyear average potential electrical energy generation in the Midwest is 4.63 ± 3.04 TWh (Fig. 2*L*). Across the climate gradient, higher values are observed in the humid (5.19 ± 2.97 TWh) and semihumid regions (3.37 ± 1.02 TWh), compared to the semiarid region (1.78 ± 1.73 TWh). This disparity is primarily driven by the greater aggregate land area available for solar panel installation in the eastern Midwest (Fig. 2*K*).

We further examine the impact of varying PV GCR, specifically 20% and 50%, on key biophysical variables (Fig. 2 *M–O*

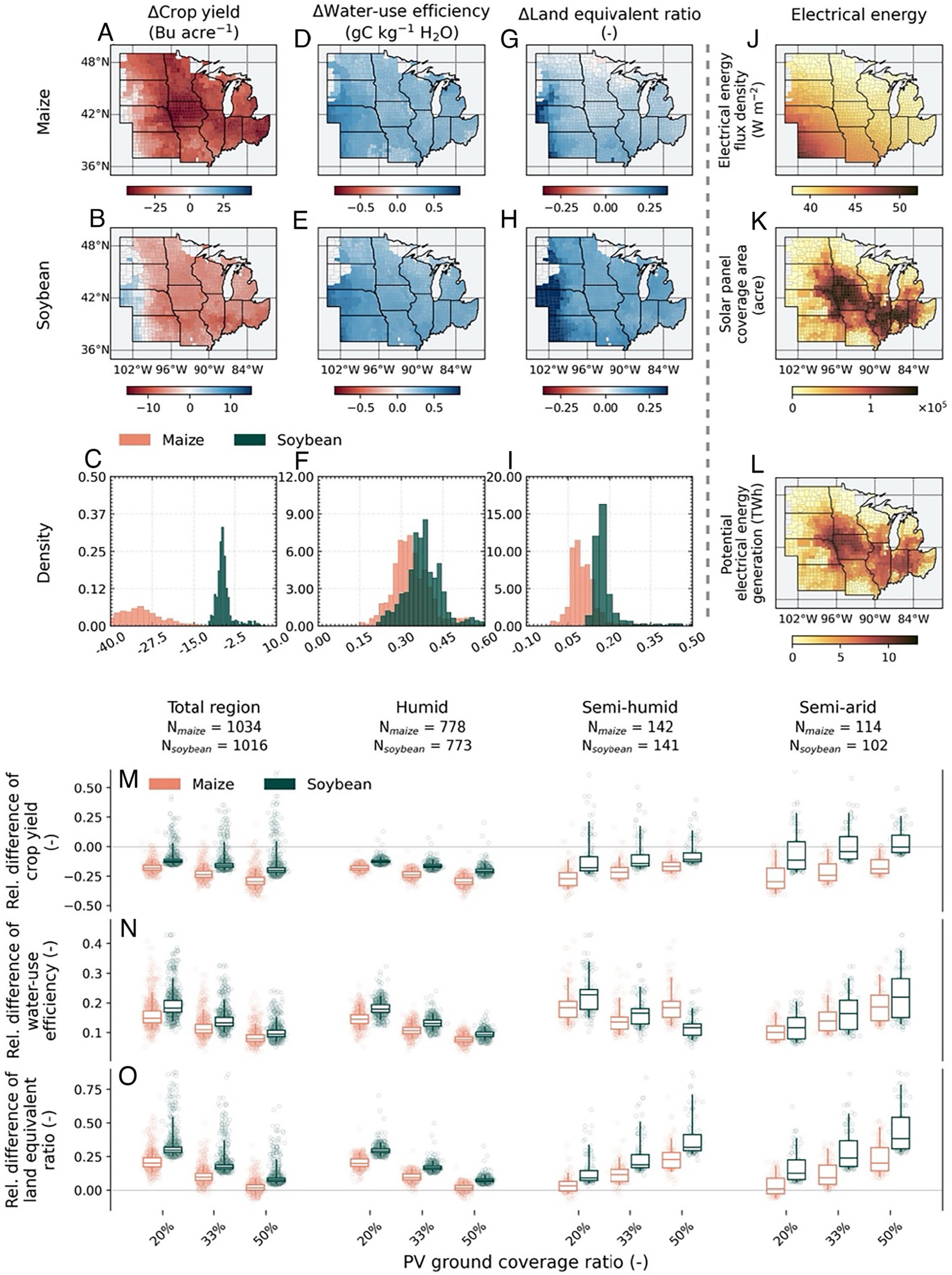

Fig. 2. Divergent impacts of agrivoltaics on biophysical feedbacks in the Midwestern United States. Multiyear (2000–2014) averaged differences between agrivoltaics and conventional agriculture: Panels (*A* and *B*) show crop yield differences for maize and soybean, (*C*) shows the frequency distribution of crop yield differences, with vertical dashed lines indicating mean values for maize and soybean. Panels(*D* and *E*) show WUE differences for maize and soybean, (*F*) shows the frequency distribution of WUE differences. Panels (*G* and *H*) show the LER differences for maize and soybean, (*I*) shows the frequency distribution of LER differences. Panels (*J*–*L*) show average electrical energy flux density (W m^{-2}), total solar panel coverage area over maize and soybean croplands (acre), and gridcell-level potential electrical energy (TWh), respectively. Box plots (*M*–*O*) present the relative differences in these variables between agrivoltaics and conventional agriculture; boxes represent the 5th–95th percentile range, and horizontal lines indicate zero.

and *SI Appendix*, Figs. S5 and S6). These levels are selected for sensitivity analysis and fall within the typical 10 to 55% global range for such systems (15, 30). While optimal real-world deployment considers numerous site-specific design, environmental, and socioeconomic factors, this analysis focuses on the biophysical consequences of these selected coverage levels. Increasing PV GCR can significantly reduce crop yield, WUE, and LER for both crops across the Midwest. However, these effects are region-specific: in the semiarid region, yield losses for both crops are reduced and eventually convert to gains for soybean at high PV GCR, whereas in the semihumid region, losses for maize and soybean are mitigated, but in the humid eastern region, yield penalties for both crops intensify. In addition, WUE and LER for both crops exhibit consistent regional trends: as PV GCR rises, both metrics decline in the overall and humid regions but increase in the semiarid region; in the semihumid region, WUE decreases while LER increases. These regional disparities highlight the importance of balancing trade-offs between food, energy, water, and land outcomes when designing agrivoltaics.

Mechanisms Underlying Biophysical Divergence across Climate Gradients. To understand the mechanisms driving the contrasting biophysical impacts of agrivoltaics across the climate gradient, we use a structural equation modeling (SEM; see *Materials and Methods*) (Fig. 3). This approach enables us to trace how solar

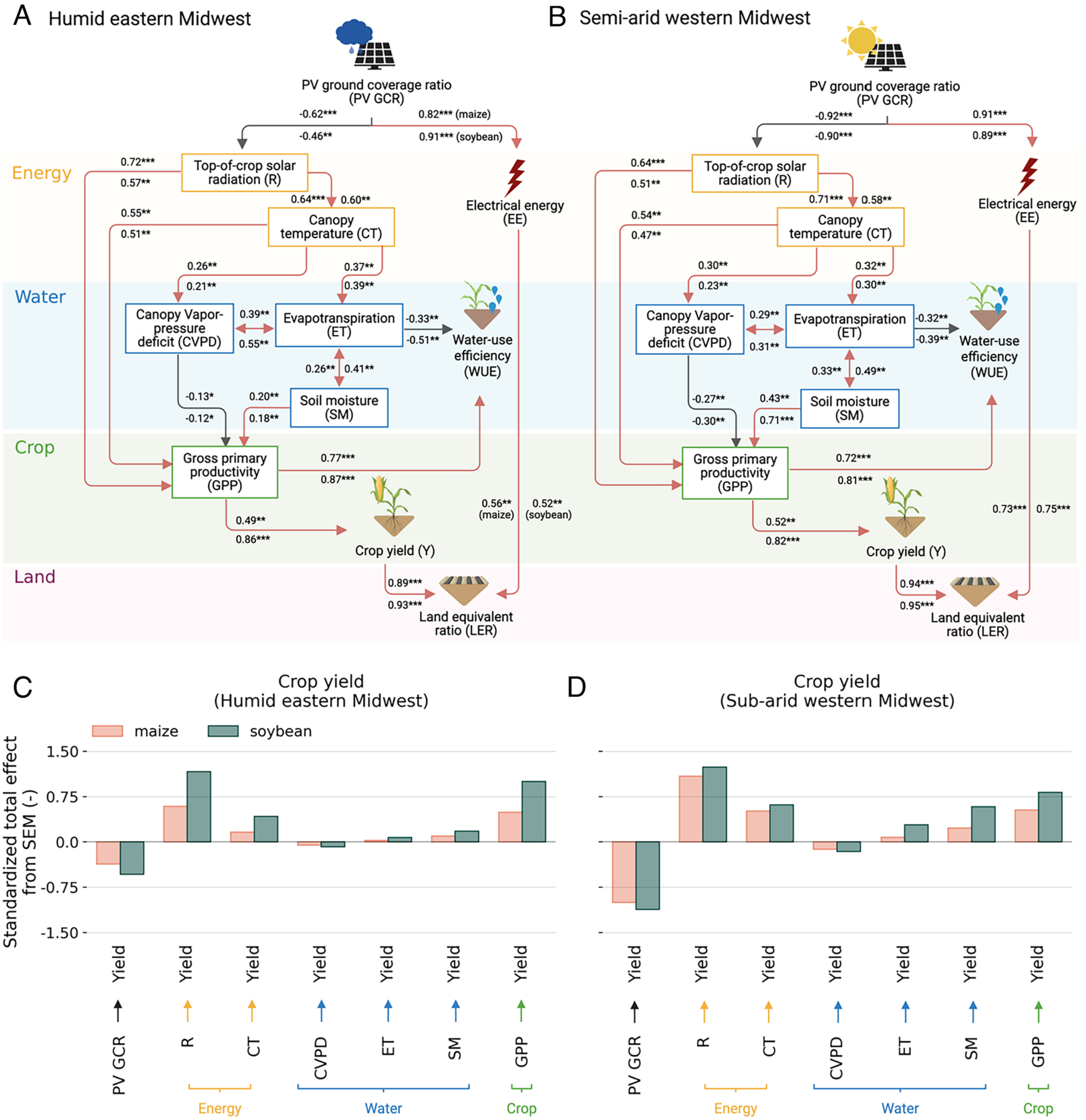

Fig. 3. Mechanisms underlying biophysical divergence under varying climate regimes. Piecewise structural equation modeling (SEM) is used to quantify the direct and indirect effects of key biophysical variables under two representative climate conditions: (*A*) humid and (*B*) semiarid. The SEM framework evaluates the influence of PV GCR, electrical energy output (EE), top-of-crop solar radiation (R), CT, CVPD, SM, ET, WUE, GPP, and crop yield (Y) on the LER. Solid red arrows denote positive pathways; solid black arrows denote negative pathways. Numbers adjacent to arrows are standardized path coefficients (comparable to regression weights). Significance levels: *$P < 0.05$, **$P < 0.01$, ***$P < 0.001$. Only significant pathways are displayed ($P < 0.05$). Goodness-of-fit statistics indicate strong model-data agreement: for panel (*A*), Fisher's C = 6.01, $P = 0.10$ (maize) and Fisher's C = 3.55, $P = 0.23$ (soybean); for panel (*B*), Fisher's C = 2.10, $P = 0.34$ (maize) and Fisher's C = 3.20, $P = 0.39$ (soybean). (*C* and *D*) Standardized total effects (direct + indirect) for crop yield under humid (*C*) and (*D*) semiarid conditions.

panels alter key energy, water, and crop variables ultimately influencing crop yields, WUE, LER, and electrical energy in both maize- and soybean-based agrivoltaics. All models are statistically robust (Fisher's C > 0.05 and $P < 0.05$), confirming their strong representation of the investigated relationships.

Light limitation prevails in the humid eastern Midwest: in areas where energy typically limits plant growth, the SEM explains 44% and 41% of the variance in maize and soybean yields, respectively. Increased PV GCR directly boosts electrical energy generation (standardized coefficient, $r = 0.82$ for maize; $r = 0.91$ for soybean) but markedly reduces the solar radiation reaching the crop canopy ($r = -0.62$; $r = -0.46$). The reduced radiation lowers CT ($r = 0.64$; $r = 0.60$), and this combined decline in light availability and canopy warmth emerges as the primary constraint on photosynthesis, ultimately decreasing GPP in both crops. Consequently, the lower GPP translates into reduced crop yields ($r = 0.49$; $r = 0.86$) and diminished WUE ($r = 0.77$; $r = 0.87$), despite concurrent decreases in ET. However, the substantial gains in electrical energy partially offset these agricultural losses, leading to improved LER when crop and energy outputs are jointly considered.

Water conservation prevails in semiarid western Midwest: in regions where water scarcity primarily constrains plant growth, the SEM accounts for 43% and 40% of yield variance for maize and soybean, respectively. While solar panels similarly reduce incoming radiation and increase electrical energy generation, the shading effect benefits crops by lowering ET and moderating CT. The resulting decrease in CVPD ($r = -0.27$; $r = -0.30$) and increase in SM ($r = 0.43$; $r = 0.71$) improve plant water availability, enhancing stomatal conductance and significantly increasing GPP. This moisture-driven productivity enhancement largely compensates for potential yield losses from reduced solar radiation, demonstrating how agrivoltaic benefits depend critically on regional water availability. In this water-limited environment, SEM further reveals that stomatal conductance exerts stronger positive effects on productivity and yield in C_3 soybean than C_4 maize, indicating that agrivoltaic microclimates provide greater relative benefits to C_3 crops in water-limited environments.

Divergent Economic Incentives of Agrivoltaics. We next analyze the profitability of agrivoltaics across the Midwestern United States under current climate conditions (2000–2014), considering outcomes for both farmers and solar developers. With agrivoltaics, the farmers retain profits ($\pi_{F,AgPV}$) from both grain sale and land lease revenue from the solar developers, whereas the solar developers own the generated electricity and its associated profits ($\pi_{SD,AgPV}$) (*Materials and Methods*). For a scenario with the base economic parameters and a PV GCR of 33%, we first assess the economic impact on farmers by analyzing the change in their profitability from agrivoltaics relative to conventional agriculture ($\Delta\pi_F = \pi_{F,AgPV} - \pi_{SD,AgPV}$) (Fig. 4 *A* and *B*). This analysis reveals distinct regional differences in $\Delta\pi_F$ across the entire region. For maize, agrivoltaics consistently reduce farmer total profits ($\Delta\pi_{F\_maize} < 0$). This profit reduction is relatively modest in the semiarid west (−6% compared to conventional agriculture) but more substantial in the humid east (−16%). In contrast, soybean profitability under agrivoltaics exhibits a divergent regional response: farmers in the semiarid west achieve a 9% profit increase ($\Delta\pi_{F\_soybean} > 0$), while those in the humid east face a 2% reduction in profit ($\Delta\pi_{F\_soybean} < 0$). These regional variations in $\Delta\pi_F$ are positively associated with agrivoltaic-induced changes in crop yields.

Besides, we evaluate the economic impact on solar developers by comparing their profitability relative to standalone solar ($\Delta\pi_{SD} = \pi_{SD,AgPV} - \pi_{SD,PV}$) (Fig. 4 *C* and *D*). Our analysis reveals that agrivoltaics reduce solar developer total profits ($\Delta\pi_{SD} < 0$) across most Midwestern counties: 82.30% for maize (comprising 78.24% + 4.06%) and 86.02% for soybean (53.74% + 32.28%). However, a small fraction of counties experience increased total profits ($\Delta\pi_{SD} > 0$): 17.70% for maize (16.73% + 0.97%) and 13.98% for soybean (3.94% + 10.04%). These widespread profit reductions arise from a combination of diminished electricity revenue and elevated infrastructure costs. Compared to standalone solar, agrivoltaics generate lower multiyear average revenues, with the effect most pronounced in eastern counties (*SI Appendix*, Fig. S7 *A* and *B*). Simultaneously, the levelized costs of energy (LCOE) increases substantially due to the additional infrastructure required to integrate agriculture with solar installations (*SI Appendix*, Fig. S7 *C* and *D*). In addition, per-acre farmer profits follow spatially divergent patterns similar to total profits, whereas per-acre solar developer profits are nearly uniform across regions (*SI Appendix*, Fig. S8). Normalizing by land area for maize and soybean isolates economic viability from land availability, providing a scale-independent metric to evaluate outcomes across different deployment scenarios.

We further examine the economic trade-offs of adopting agrivoltaics relative to conventional agriculture or standalone solar systems (Fig. 4 *E* and *F*). All 1,034 Midwestern counties are classified into four profitability categories based on whether agrivoltaics increase or decrease profits relative to conventional agriculture ($\Delta\pi_F$) or relative to standalone solar ($\Delta\pi_{SD}$): a win-win scenario where both farmers and solar developers gain ($\Delta\pi_F > 0$, $\Delta\pi_{SD} > 0$; F+ SD+); two trade-off scenarios favoring either solar developers ($\Delta\pi_F < 0$, $\Delta\pi_{SD} > 0$; F− SD+) or farmers ($\Delta\pi_F > 0$, $\Delta\pi_{SD} < 0$; F+ SD−); and a lose-lose scenario where both incur losses ($\Delta\pi_F < 0$, $\Delta\pi_{SD} < 0$; F− SD−). For maize-based agrivoltaics, we observe a clear west-to-east reduction in overall economic viability. In the semiarid western region, 38.6% of counties show profits for solar developers but losses for farmers (F− SD+), while 21.1% of counties display the opposite (F+ SD−); the remainder mostly experience mutual losses (F− SD−). In contrast, in more humid regions, losses for both stakeholders dominate: 71.1% of semihumid middle counties and 85.9% of humid eastern counties show F− SD− outcomes. Soybean-based systems exhibit a significantly more favorable economic profile across all regions. In the semiarid western region, 98% of counties benefit farmers, with 64.7% of counties favoring farmers alone (F+ SD−) and 33.3% of counties create win-win scenarios (F+ SD+). This positive pattern extends partially into the semihumid middle region, where 58.9% of counties still favor farmers despite developer losses (F+ SD−). In the humid east, conditions worsen, with 65.9% of counties experiencing mutual losses (F− SD−) for both stakeholders. These findings suggest two critical patterns: first, soybean consistently outperforms maize in economic viability for agrivoltaics across all climate regions; second, regardless of crop choice, the semiarid western region provides the most economically favorable conditions for agrivoltaic implementation.

The economic incentives for agrivoltaic adoption are highly sensitive to market fluctuations. We conduct sensitivity analyses for key parameters for both total-area and per-acre profits: crop prices and land lease rates for farmers, and power purchase agreement (PPA) prices for solar developers (*Materials and Methods*). Farmers' profitability ($\Delta\pi_F$) is primarily determined by crop prices and land leasing fees. Lower crop prices and higher lease fees both increase $\Delta\pi_F$, shifting more counties toward win-win (F+ SD+) or farmer-favored trade-off (F+ SD−) scenarios (*SI Appendix*, Figs. S9–S12). Solar developers' profitability ($\Delta\pi_{SD}$) is governed mainly by the PPA price, where higher values increase $\Delta\pi_{SD}$ and move additional counties toward win-win (F+ SD+) or solar developer-favored

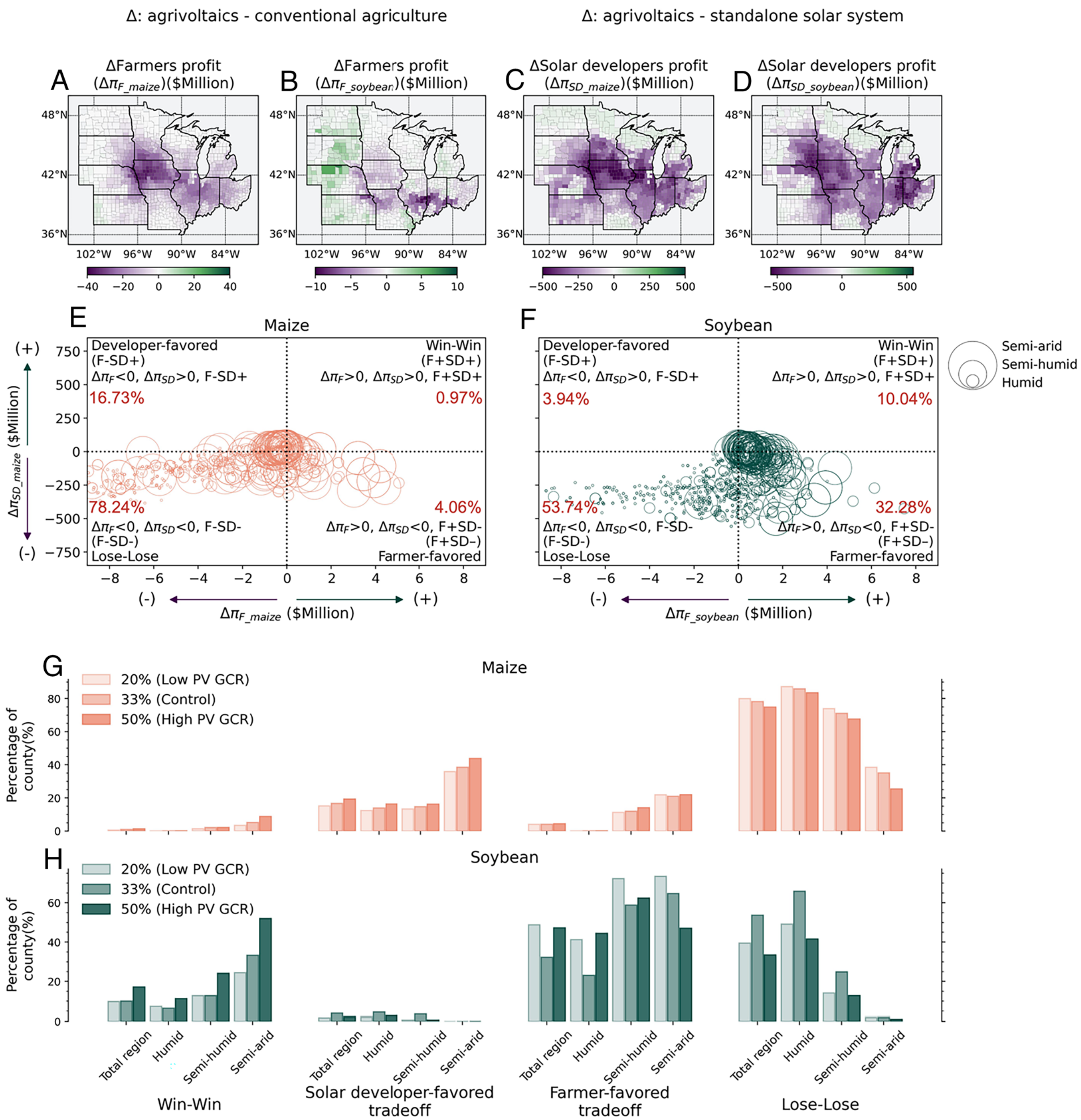

Fig. 4. Divergent impacts of agrivoltaics on economic outcomes for farmers and solar developers in the Midwestern United States for a scenario with base economic parameters and a PV GCR of 33%. Multiyear (2000 to 2014) averaged differences between agrivoltaics and conventional systems in (*A* and *B*) farmers' profitability ($\Delta\pi_F$) relative to conventional agriculture, and (*C* and *D*) solar developers' profitability ($\Delta\pi_{SD}$) relative to standalone solar systems. Panels (*E* and *F*) classify outcomes into four quadrants: "win-win" (F+ SD+), "trade-off" (F− SD+ or F+ SD−), and "lose-lose" (F− SD−). Note that proportions shown in red denote the exact shares across the four profitability scenarios. Circle sizes represent climate zones, large: semiarid, medium: semihumid, small: humid. Panels (*G* and *H*) show the percentage of counties for maize and soybean falling into each scenario under high, control, and low photovoltaic ground coverage ratio.

trade-off (F− SD+) scenarios (*SI Appendix*, Figs. S13 and S14). We further identify the market thresholds required for agrivoltaics to achieve parity, with conventional agriculture for farmers and with standalone solar systems for solar developers (*SI Appendix*, Fig. S15). Maize requires substantially higher crop prices than soybean to reach profit equivalence with conventional farming, but correspondingly lower land lease thresholds. For the two agrivoltaic systems, the PPA break-even thresholds are substantially below those of standalone solar systems, highlighting the economic challenges of achieving profitability parity under current market conditions. Additionally, we assess the influence of PV GCR on economic incentives for adoption, with a focus on the semiarid western region (Fig. 4 *G* and *H*). Our analysis of PV GCR in the context of win-win outcomes indicates that, for both maize- and soybean-based agrivoltaics, increasing panel coverage progressively increases the proportion of win-win counties (F+ SD+) across the Midwest and within each climate zone. This effect is most pronounced in semiarid regions, where increased shading alleviates crop water stress while additional panels, combined with abundant solar resources, enhance electricity generation.

Future Climate Reduces Regional Disparities in Agrivoltaic Outcomes. Finally, we evaluate the impact of future climate change on agrivoltaics at mid-century (2040–2054) and end-of-century (2086–2100) across the Midwest under three climate scenarios from Coupled Model Intercomparison Project Phase 6 (CMIP6): SSP1-2.6, SSP3-7.0, and SSP5-8.5. Multimodel ensemble models (*Materials and Methods*) project significant warming by 2100 compared to 2000–2014 baselines (*SI Appendix*, Fig. S16). By 2100, annual mean 2-m air temperatures are projected to increase to approximately 11.2 °C (+9%) under SSP1-2.6, and to 14.9 °C (+43%) and 15.8 °C (+55%) under SSP3-7.0 and SSP5-8.5, respectively. Precipitation projections remain uncertain, showing slight spring (April–May) increases about 500 mm y^{-1} (+1%) under SSP1-2.6 and SSP3-7.0, and 520 mm y^{-1} (+0.3%) under SSP5-8.5, contrasted by mid-summer (July–August) declines of 3 to 5% across all scenarios. Surface solar radiation flux is projected to reach 179.25 W m^{-2} (+1%), 175.81 W m^{-2} (+0.1%) and 176.03 W m^{-2} (+0.04%) under SSP1-2.6, SSP3-7.0, and SSP5-8.5, respectively. The climate projections indicate a substantial eastward expansion of semiarid conditions across the Midwest by 2100, based on model-based estimates of the aridity index (Fig. 5 *A–C* and *SI Appendix*, Fig. S17). Relative to the 2000–2014 baseline, the area of semiarid cropland is projected to increase modestly by 5.3% under SSP1-2.6, reaching 101,822 km^2 (8.46% of total cropland). Under higher emission scenarios, however, this expansion accelerates markedly: SSP3-7.0 projects a 21.6% increase to 165,820 km^2 (13.77%), while SSP5-8.5 forecasts a striking 174% expansion to 373,640 km^2 (31.04%).

Climate change is projected to reshape conventional agriculture across the Midwest by 2100 (*SI Appendix*, Figs. S18 and S19). Under the SSP1-2.6, maize and soybean yields remain comparable to the baseline (2000–2014), with reduced productivity in the semiarid western Midwest and higher yields in the east. Under the SSP3-7.0 and SSP5-8.5, however, yield reductions intensify and extend eastward, leaving only the far eastern Midwest with relatively high yield by 2100. These climate scenarios also fundamentally alter yield differences between agrivoltaics and conventional agriculture through 2100. While agrivoltaics show significant yield penalties relative to conventional agriculture during the baseline period (2000–2014), particularly for maize, this gap narrows as climate stress intensifies. As water limitation becomes more widespread, the relative benefit of shading-induced moisture conservation increases, leading regional yield penalties to diminish or even reverse (*SI Appendix*, Figs. S20 and S21). For maize under SSP5-8.5, the yield penalty decreases from −16.41 ± 8.47 Bu/acre (2040–2054) to −10.35 ± 6.91 Bu/acre (2086–2100). Notably, soybeans shift from yield penalty to gains under SSP5-8.5, agrivoltaic soybean yields exceed conventional agriculture by 5.35 ± 4.91 Bu/acre (2040–2054), increasing to 7.97 ± 4.16 Bu/acre (2086–2100). Besides, WUE in agrivoltaics show consistent improvements relative

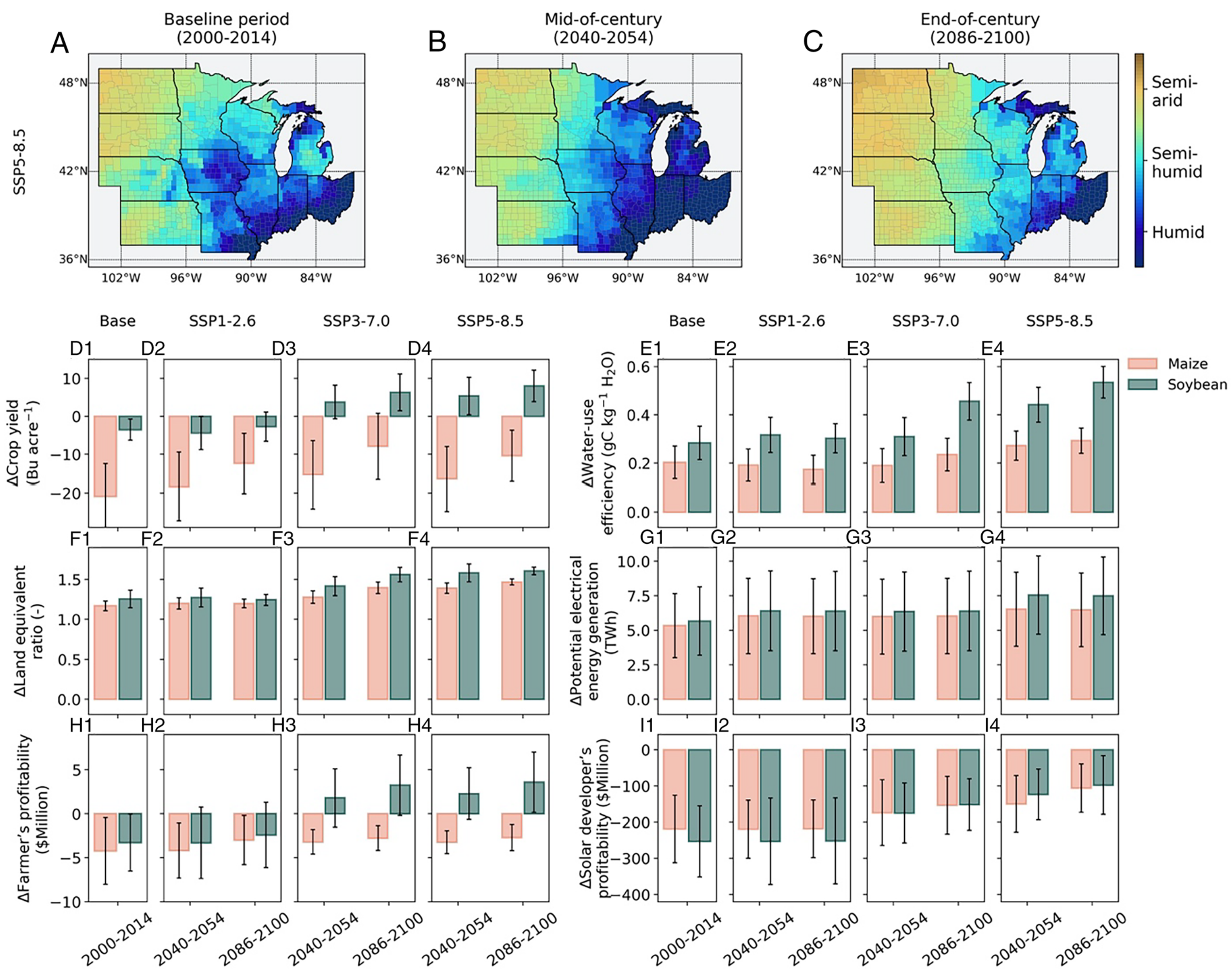

Fig. 5. Projected impacts of climate change on the biophysical and economic outcomes of agrivoltaics in the Midwestern United States for a scenario with base economic parameters and PV GCR of 33%. Panels (*A–C*) show hydroclimatic classifications of the US Midwest including semiarid, semihumid, and humid during the (*A*) baseline period (2000–2014), (*B*) mid-century (2040–2054), and (*C*) end-century (2086–2100) under SSP5-8.5. Multiyear average differences between agrivoltaics and conventional systems in (*D1–D4*) crop yield, (*E1–E4*) WUE, (*F1–F4*) LER, (*G1–G4*) potential electrical energy generation, (*H1–H4*) farmers' profitability, and (*i1–i4*) solar developers' profitability across three climate scenarios and time periods.

to conventional agriculture over time (Fig. 5, e1-e4). LER similarly increases, with projected gains widening through the century (Fig. 5, f1-f4). Electrical energy generation also shows positive trends across all climate scenarios (Fig. 5, g1-g4), with advantages reaching 12.38±5.43 TWh, 12.41±5.46 TWh, and 12.13±5.32 TWh under SSP1-2.6, SSP3-7.0, and SSP5-8.5, respectively.

For farmers, profitability changes ($\Delta\pi_F$) vary significantly by climate scenario. Under the SSP1-2.6 scenario, farmer profitability remains relatively stable near baseline levels for both maize and soybean through 2100 (Fig. 5, h1-h2 and *SI Appendix*, Fig. S22). However, under SSP3-7.0 and SSP5-8.5, farmer profitability consistently improves over time, particularly for soybean (Fig. 5, h3-h4). For instance, under SSP5-8.5, soybean farmers across the regions could see their profit advantage increase from $1.99 million by 2054 to $3.81 million by 2100, representing a 69.43% improvement in the profit differential compared to current climate conditions. Further examination of spatial patterns reveals that by 2100, farmer profitability for maize and soybean increases in the western Midwest and progressively expands eastward into the central Midwest, whereas the eastern Midwest experiences still reduced profitability for both crops (*SI Appendix*, Fig. S22). It suggests that the zone of farmers' advantage stays largely in the same western regions but becomes more profitable. The advantage in the central Midwest gradually increases, but the advantage in the east remains negligible. For solar developers, agrivoltaics generally remain less profitable than standalone solar installations ($\Delta\pi_{SD}$), though this disadvantage diminishes under higher emission scenarios (Fig. 5, i1-i4 and *SI Appendix*, Fig. S22). By 2054, solar developer losses are projected to decrease to approximately $273-348 million under SSP3-7.0 and SSP5-8.5. By 2100, these losses further decrease to $203-305 million under the respective scenarios, indicating a gradual improvement in the economic viability of agrivoltaics for energy producers as climate conditions evolve.

Discussion

Rising global food and energy demands are intensifying competition for land, highlighting the need for multifunctional land use. Agrivoltaics, the colocation of agriculture and solar energy production, offers a promising dual-use strategy, yet its benefits are uncertain across climate-diverse regions like the Midwestern United States, a nation's breadbasket and an emerging renewable energy hub. In this study, we highlight significant divergent impacts of agrivoltaics on biophysical feedbacks and economic incentives across the Midwestern climate gradient. Our findings indicate that agrivoltaics fail to deliver consistent benefits throughout the region without careful consideration of climate gradients, crop choice, and system design parameters. However, using future climate projections, we find a potential narrowing of regional disparities due to eastward expansion of semiarid conditions across the Midwest. In such water-limited environments, agrivoltaics are likely to become more beneficial, offering stronger synergies for sustainable land use. These findings provide potential guidance for policymakers, land managers, and investors aiming to scale agrivoltaics in ways that are both regionally appropriate and climate resilient.

Agrivoltaics generate significant biophysical divergences across the Midwestern United States, primarily due to the region's strong west-to-east climate gradient. These divergent feedbacks align with Liebig's Law of the Minimum (31, 32), which posits that plant growth is constrained not by total resources but by the scarcest resource. The microclimatic effects of solar panels exhibit distinct spatial patterns across the climatic gradient. In the water-limited western region, water availability represents the primary limiting factor, and solar panel shading serves as a way to reduce plant stress by reducing evapotranspiration, moderating air-ground temperatures, and conserving soil moisture. Thus, the reduced solar radiation is outweighed by improved water conservation, shifting the limiting factor equation. Conversely, in the cooler, more humid eastern regions where water is abundant, light availability becomes the limiting factor, and panel shading negatively impacts photosynthetic potential and thus potentially inhibiting crop growth. Our findings complement and extend earlier site-specific studies (33, 34). Earlier studies have documented enhanced crop production or resource-use efficiency under agrivoltaics in water-limited ecosystems like Arizona (USA) (10, 35) and Herdwangen-Schönach (Germany) (36), while yield reductions have been observed for some crops in well-watered environments (e.g., Chengdu, China) (37). Our findings highlight the particular suitability of agrivoltaics for water-limited ecosystems, thereby providing a strong evidence-based rationale for prioritizing their deployment in arid and semiarid regions. This contrasts with the broader Midwestern context where, for instance, average crop yields from agrivoltaics cannot uniformly surpass those from conventional agriculture. Critically, incorporating ecological knowledge of climate gradients and limiting factors can inform agrivoltaics design and operation, particularly when developing arrays that coprioritize renewable energy generation and sustainable farming practices.

Beyond broad climatic influences, the specific crop cultivated introduces further local variability to how agrivoltaics perform. For example, soybean (a C_3 crop) outperformed maize (a C_4 crop) in relative yield, water-use efficiency, and land equivalent ratio in the hot, water-limited western region. The differing responses are likely due to their different photosynthetic physiologies (36, 37). C_4 plants like maize, adapted for high efficiency under intense light and heat by minimizing photorespiration, could experience reduced photosynthetic potential under significant shading. Conversely, C_3 plants such as soybean, while more susceptible to photorespiration at high temperatures, can benefit from the microclimatic moderation under solar panels in hot, high-light environments. For soybean, reduced heat and light stress and lower evapotranspiration under panel shade more than offset the shading-induced loss of light, a balance not achieved by maize. Our results, showing that shade benefits certain C_3 crops in arid, stressful environments by enhancing physiological performance, align with previous findings for crops such as chiltepin peppers, jalapenos, and tomatoes (10). Future research focusing on crop-specific shade adaptation and acclimation mechanisms will be key to accurately predicting and optimizing agrivoltaics performance.

These complex biophysical outcomes translate into divergent economic realities for farmers and solar developers. Our analysis reveals that for farmers, profitability is strongly tied to a crop-specific, climate-driven pattern rooted in biophysical effects. Agrivoltaics colocated with soybean in the semiarid western Midwest demonstrate clear economic potential due to enhanced yields, but systems with both maize and soybean in the humid east typically incur net financial losses, as reduced crop revenues are not fully offset by land-lease income. Thus, soybean-based agrivoltaics could offer economic incentives in water-limited regions if maximizing farm profit is the primary goal, though even in these cases, returns remain lower than those from leasing land entirely for solar development. Additionally, given the inherent volatility of agricultural commodity prices (38), revenue from leasing land for solar energy provides a more stable and predictable income stream. Agrivoltaics can further benefit farmers by diversifying income sources and reducing financial risk, an especially attractive feature for risk-averse producers.

For solar developers, agrivoltaics are generally less economically attractive than standalone solar across the Midwest, primarily due to the higher costs of installation of panels and infrastructure needed for integrating agriculture (15, 39). Consequently, mutually beneficial (win-win) scenarios for both farmers and developers are limited to specific cases, such as soybean-based systems in the semiarid western region. This mismatch often creates an adoption dilemma: agrivoltaic designs that are profitable for one producer group may be financially unviable for the other. This tension highlights the need for targeted policy interventions to align incentives for two stakeholder groups.

Furthermore, our sensitivity analysis reveals distinct policy levers for each stakeholder group. Agrivoltaic adoption reflects a balance of opportunity costs shaped by crop prices and land lease fees: high crop prices discourage adoption, while higher lease fees incentivize it. In contrast, solar developers' profitability depends on PPA prices, independent of agricultural markets. This divergence in economic drivers explains why uniform subsidies often fail; effective policies must target these distinct levers concurrently (9). While sensitivity analysis identifies the key drivers, threshold analysis quantifies the levels required for agrivoltaics to become viable. This study defines breakeven values for land lease fees, crop prices, and PPA prices, points where each stakeholder shifts from loss to profit. Comparing these thresholds with current market conditions reveals the "incentive gap" or the minimum financial support needed to achieve profitability. This framework enables policymakers to calibrate subsidies precisely, closing viability gaps for farmers, developers, or both while avoiding oversubsidization. Future work should extend this approach to include additional stakeholders, such as agricultural lenders, rural cooperatives, and food processors, to better capture the broader incentive landscape governing agrivoltaic adoption at scale.

These biophysical and economic divergences thus paint a clear picture: the potential of agrivoltaics is unlikely to be uniformly distributed across the Midwest. Optimizing solar panel coverage to minimize negative outcomes depends heavily on local climate conditions, yet such region-specific guidance is largely lacking (40, 41). Our results underscore the need for climate-tailored design rather than a one-size-fits-all approach. In drier regions, "energy-centric" installations on water-limited cropland should be prioritized, utilizing higher solar panel density while incorporating shade-tolerant crops that benefit from the modified microclimate from agrivoltaics. In contrast, more humid regions require "agriculture-centric" approaches (42) that maintain crop yield by using lower panel densities to minimize shading. This adaptive framework embodies principles of ecological engineering, where human-built systems are designed to work synergistically with natural processes. While grounded in the Midwestern United States, this framework may apply to other climate-vulnerable regions under ecological or economic stress, such as India and China (41, 43).

Looking forward, however, these established regional divergences are not necessarily static; our projections indicate that they may significantly shift, and even narrow, as the climate continues to change. Climate projections indicate increasing water scarcity in the eastern Midwest (under the high-emission and highest-emission scenarios), suggesting that these integrated solar-agricultural systems will become increasingly beneficial in this previously less favorable region (44, 45). Without effective adaptation strategies, conventional agriculture in these areas faces significant production declines (44, 46). Our research demonstrates that agrivoltaics can effectively mitigate drought impacts, enhance crop yields, and improve water and land use efficiency throughout the Midwest. This translates to more favorable financial returns for farmers compared to conventional agriculture as climate warming. While agrivoltaics currently show lower profitability than standalone solar installations, our projections indicate this gap will progressively narrow over time. This economic trajectory suggests that "dual-use" agrivoltaics will increasingly compete with "single-purpose" photovoltaics, promoting adoption by farmers and solar developers seeking climate resilience and income diversification. Supportive future policies, such as incentives and streamlined permitting, could further accelerate deployment. However, we acknowledge several limitations to our projections. First, our modeling does not account for potential land-atmosphere feedback effects from large-scale agrivoltaics (47). When deployed over sufficiently large areas, these systems may influence local rainfall patterns and temperature regimes by altering energy and water exchanges (48). Future research should investigate these feedbacks to improve regional climate projections and assess the full environmental impact of widespread agrivoltaics. Second, although we account for market price sensitivity when assessing current profitability for both farmers and solar developers, our future economic projections assume static prices for electricity, photovoltaic components, and agricultural products. This simplification reduces realism, as future outcomes will likely depend on such as raw material costs and evolving policy environments (e.g., subsidies, tariffs) (10, 49). Incorporating dynamic market models and policy scenarios in future analyses would yield more robust economic forecasts for agrivoltaics under changing climate conditions.

In summary, our integrated modeling framework quantifies how climate drives divergent biophysical and economic impacts of agrivoltaics. We find that agrivoltaics currently offer greater synergistic benefits across food, energy, water, and economics in the semiarid western Midwest compared to the more humid eastern regions. However, this prevailing regional disparity is projected to diminish under modeled climate change scenarios. This evolving climatic landscape can, in turn, transform initially challenging agrivoltaic prospects into broadly positive ones, fostering more widespread dual land use and enhancing food-energy synergies throughout the entire Midwest. Ultimately, our holistic framework provides a robust and economically grounded foundation for designing effective, region-specific strategies to scale agrivoltaics in a rapidly changing world.

Materials and Methods

Integrated Biophysical–Economic Modeling Framework. We develop an integrated biophysical–economic modeling framework to assess how the current and projected climate conditions influence the biophysical and economic outcomes of agrivoltaics in the Midwestern United States. The framework begins with a regional-scale biophysical model explicitly designed to capture the impacts of agrivoltaics on energy, water, and plant-soil dynamics. A benefit–cost analysis is then used to evaluate the economic feasibility of agrivoltaic adoption, and to quantify its potential profitability for both farmers and solar developers. The following sections detail the algorithms and methodologies underpinning this comprehensive modeling approach.

Land Model. CLM5 (50) is a state-of-the-art land model and serves as the land component of Community Earth System Model (CESM) version 2 (51). Biophysical and biogeochemical processes are simulated separately for each subgrid land unit, column, and plant functional type, with all units sharing the same atmospheric forcing. Surface variables and fluxes are area-weighted averages of subgrid quantities. This study simulates key processes including land-type heterogeneity, radiation, turbulent fluxes, soil hydrology, plant hydraulics and physiology, carbon and nitrogen cycling, and plant growth. Of particular relevance to this study is the capability of CLM5 to explicitly represent agriculture. The CLM5 crop module, derived from Agro-IBIS (52), has been enhanced to simulate actively managed croplands worldwide (53). It includes multiple crop functional types (e.g., temperate and tropical maize and soybean) and dynamically represents phenology, carbon allocation to grain and structural pools, and management practices such as planting and fertilization. Crop yields are mechanistically derived from photosynthesis and carbon allocation. C_3 photosynthesis follows the Farquhar model with temperature acclimation (54, 55), while C_4 photosynthesis uses the Collatz formulation (56). Stomatal conductance is calculated using the Medlyn formulation (57), accounting for water and nitrogen limitations. Soil biogeochemistry is represented through a vertically resolved decomposition cascade that conserves carbon, nitrogen, water, and energy during land-use and management transitions (58, 59). Detailed descriptions of these processes are available in ref. 60. However, the default CLM5 does not support the simulation of agrivoltaics and their interactions with dynamic ecosystems.

Agrivoltaics Model. To simulate the impact of agrivoltaics on food–energy–water nexus, an agrivoltaics model is integrated into the CLM5 (referred to CLM5-AgPV) (61). To our knowledge, most, if not all, agrivoltaic models inadequately represent how biophysical and biogeochemical processes responses to agrivoltaics, primarily due to the limitations of rigid frameworks. Although a few modeling studies examine how solar panels create shade and alter microclimates, they often ignore changes to complex carbon cycle and crop growth (14), limiting insights into synergies among food production, renewable energy, and water conservation. In this study, we develop the CLM5-AgPV model by extending the subgrid heterogeneity framework, incorporating rainfall redistribution by solar panels (62), refining surface roughness (63), and integrating the electrical energy budget into the surface energy budget (64) of CLM5 (*SI Appendix*, Figs. S23–25). Detailed information on model formulations can be found in the Supplementary Text: CLM5-AgPV model development.

Economic Model. We next integrate a benefit–cost analysis (15) with CLM5-AgPV, which allows us to assess the profitability of agrivoltaics compared to conventional agriculture (crop-only) or standalone solar systems (PV-only). We estimated annual net profits per acre from crop production and electricity generation for agrivoltaics ($\pi_{F,AgPV}$ and $\pi_{SD,AgPV}$), conventional agricultural ($\pi_{F,CA}$), and standalone solar systems ($\pi_{SD,PV}$). For crop production, profits account for yield, crop price, variable and fixed costs, and land-lease expenses, with all economic parameters specified. The agrivoltaic configuration assumes that a fraction of each acre is allocated to solar panels, with the remainder cultivated, and no buffer area reserved. For electricity generation, net profits are calculated from annual electricity production, power purchase agreement prices, renewable energy credits, and the levelized cost of energy. Model formulation and parameterization are detailed in *SI Appendix, Supplementary Text: Economic Model Development*, with a full list of parameters provided in *SI Appendix*, Table S1. For farmers, agrivoltaic adoption depends on whether profitability exceeds the threshold at which net returns surpass those from conventional agriculture. For solar developers, adoption similarly requires net returns greater than those from standalone solar installations. These distinct economic thresholds define adoption decisions for each stakeholder group and are consistent with approaches used in previous studies (39).

Field Measurements and Model Evaluation. Our comprehensive validation follows a multistep, multiscale framework. First, we perform an extensive, multiscale evaluation of the CLM5 model to establish its reliability in simulating agricultural processes. At the site scale, we select two AmeriFlux network sites that represent different climate and soil conditions for maize and soybean across the Midwestern United States. Specifically, we use comprehensive eddy-covariance data from the US-Ne3 site (University of Nebraska-Lincoln, Mead) and US-Ro1 site (Minnesota), obtaining GPP, net ecosystem exchange (NEE), and ecosystem respiration (R_{eco}) from FLUXNET2015 Tier 1 (US-Ne3) and AmeriFlux Level 2 (US-Ro1) datasets (*SI Appendix*, Fig. S26). At the regional scale, we benchmark model performance using county-level rainfed yield data from the USDA NASS and the high-resolution (30 m) daily SLOPE GPP dataset (*SI Appendix*, Figs. S27 and S28), providing a robust assessment of model fidelity. Furthermore, we conduct a dedicated, site-specific validation of the CLM5-AgPV model. We select two representative agrivoltaic field sites characterized by contrasting environmental conditions. The first one is Solar Farm 2.0 in Champaign, Illinois (40.07°N, 88.18°W) representing temperate climate conditions, where we collect soybean yield and aboveground biomass measurements (*SI Appendix*, Fig. S29 *A* and *B*). The second site is Jack's Solar Garden in Longmont, Colorado (40.16°N, 105.07°W), which experiences a semi-arid climate with a mean annual temperature of 9.7 °C and mean annual precipitation of 365 mm. Beneath the panels, perennial C_3 grasses are grown, with measurements including PPFD, soil moisture, and NPP (*SI Appendix*, Fig. S29 *C–H*). While this site represents grassland rather than cropland and lies outside our primary study region (US Midwest), it provides the only accessible long-term dataset for agrivoltaics validation in North America. To our knowledge, no comparable observational datasets exist for agrivoltaics over cropping systems in the US Midwest. Despite ecological and geographic differences, Jack's Solar Garden remains a critical site for assessing model credibility. Our ongoing fieldwork across multiple locations aims to support future refinement and validation of CLM5-AgPV. Detailed information on plant characteristics and agrivoltaics for the two sites is available in refs. 17 and (65), respectively. All model-observation comparisons are evaluated using the coefficient of determination and rms error.

Simulation Experiment Design. We use the CLM5 with agrivoltaic capabilities (CLM5-AgPV) to perform offline simulations assessing food–energy–water interactions under agrivoltaics. Our study focuses on maize and soybean production across the Midwestern United States (25°N-53°N, 83°W-104°W) at a spatial resolution of 0.47° × 0.63°. The region satisfies key criteria for agrivoltaic deployment, characterized by extensive, contiguous croplands and gentle topography suitable for both agriculture and solar development. Within each county, terrain with slopes <10° constitutes the dominant land area, while slopes >10° represent only a minor fraction. It also receives ample solar radiation, with mean global horizontal irradiance of 3.97 kWh m^{-2} day^{-1}, exceeding commonly used thresholds (>3 kWh m^{-2} day^{-1}) for efficient electricity generation (*SI Appendix*, Fig. S30). Moreover, several states, including Illinois and Minnesota, are advancing dual-use solar through supportive policies (13). In the simulations, solar panels are configured exclusively over existing maize and soybean croplands, with panel coverage levels varying across scenarios. We exclude agrivoltaics over irrigated maize and soybean systems because a) irrigation accounts for only a small fraction (~13%) of maize and soybean cropland in the Midwest, and b) integrating solar infrastructure with large-scale irrigation systems, such as center pivots, poses substantial engineering and economic challenges that merit dedicated future investigation. Accordingly, our analysis focuses on the region's extensive rainfed agroecosystems, which dominate Midwestern agriculture and are most representative of large-scale deployment potential of agrivoltaics. The paired offline simulations are used to compare the biophysical and economic outcomes from conventional agriculture and agrivoltaics over rainfed maize and soybean land across the climate gradient in the US Midwest. Model parameterization incorporates soil properties from the International Geosphere-Biosphere Programme datasets (66) and crop-specific physiological parameters validated against field observations.

Our simulation experiments employ a systematic, multistep design. First, a 70-year model spin-up (1929–1999) is performed to achieve quasi-equilibrium in carbon, water, and energy states for subsequent analysis. Second, for the current period (2000–2014), we conduct a control simulation representing conventional agriculture (crop-only, no solar panels) using climate forcing from the Global Soil Wetness Project Phase 3 (GSWP3) (67). Third, we simulate agrivoltaics over the same 2000–2014 period, testing solar panel ground coverage ratios of 20%, 33%, and 50% to reflect realistic deployment ranges. For each scenario, we assess biophysical and economic impacts of agrivoltaics across the regions. To capture market dynamics, we conduct a sensitivity analysis to evaluate how changes in economic parameters affect the profitability of farmers and solar developers during 2000–2014. Three key parameters, crop price, land leasing fee, and PPA price, are varied based on their central roles in determining economic outcomes. This analysis explores a realistic range of market conditions and their implications for the economic viability of agrivoltaics. Finally, land-use scenarios, including conventional agriculture and agrivoltaics, are projected from 2015 to 2100 using CMIP6 data (68–73). Detailed information can be found in the *SI Appendix, Supplementary Text: Future Climate*. Note that our model does not explicitly incorporate potential land-use transitions under future climate conditions, such as the potential emergence of abandoned or marginal lands in the western U.S. Midwest, as this would require additional assumptions about land-use dynamics beyond the scope of this study.

Causal Analysis. To disentangle the direct and indirect effects of agrivoltaic design on energy, water, food, and land outcomes, we use a piecewise structural equation modeling (SEM) to quantify the causal relationships among photovoltaic ground coverage ratio, top-of-crop radiation, canopy temperature, evapotranspiration, canopy vapor-pressure deficit, soil moisture, water-use efficiency, GPP, crop yield, electrical energy generation, and land equivalent ratio across semiarid and humid climate zones. We first construct a hypothesized conceptual model (*SI Appendix*, Fig. S31 and Table S3) that include all reasonable pathways. Nonsignificant paths and variables are then sequentially removed until only statistically significant relationships remain and/or model fit ceased to improve, as indicated by the minimization of the Akaike Information Criterion (AIC) (74). Model fit is evaluated using Fisher's C test (75). To assess model explanatory power and hypothesis significance, we calculate R^2 values for maize and soybean yield. Upon achieving satisfactory model fit, we interpret the standardized path coefficients and their associated *P* values, where each coefficient represents the strength and direction of the partial relationship between two variables. The SEM is conducted in R package *piecewiseSEM* (version 2.3.0) (76).

Data, Materials, and Software Availability. The NCAR Community Land Model version 5.0 (CLM5.0) is available on GitHub: https://github.com/ESCOMP/ctsm (50). The developed agrivoltaics model (CLM5-AgPV) is deposited on Figshare (77). Measurement datasets from two agrivoltaic sites, Solar Farm 2.0 in Champaign, Illinois, and Jack's Solar Garden in Longmont, Colorado, are archived on Figshare (78). FLUXNET2015 dataset is available at http://fluxnet.fluxdata.org/data/fluxnet2015-dataset/. NLDAS-2 forcing dataset can be accessed at https://ldas.gsfc.nasa.gov/nldas/nldas-2-forcing-data, and GSWP3v1 dataset at https://search.diasjp.net/en/dataset/GSWP3_EXP1_Forcing. Remote sensing SLOPE GPP data are obtained by ref. 79, and maize and soybean yield data are provided by the USDA at https://quickstats.nass.usda.gov/.

ACKNOWLEDGMENTS. We sincerely thank Prof. Elizabeth A. Ainsworth at the University of Illinois Urbana-Champaign, for her insightful feedback on an earlier draft. We acknowledge the valuable technical support from Dr. Keith Oleson and Dr. Samuel Levis at NSF National Center for Atmospheric Research (NSF NCAR). This work is funded by the US Department of Agriculture's National Institute of Food and Agriculture through the Sustainable Agricultural Systems project entitled "Sustainably Co-locating Agricultural and Photovoltaic Electricity Systems (SCAPES)," led by the University of Illinois Urbana-Champaign, grant number: 2021-68012-35898. We also acknowledge funding support from the NSF CAREER Award (grant number: 1847334). Computation resources for this work are supported by the University Allocations Program of the Computational and Information Systems Laboratory (CISL), NSF NCAR through the NSF Career grant to Agroecosystem Sustainability Center (ASC).

Author affiliations: [a]Agroecosystem Sustainability Center, Institute for Sustainability, Energy, and Environment, University of Illinois Urbana-Champaign, Urbana, IL 61801; [b]Department of Crop Sciences, College of Agricultural, Consumer and Environment Sciences, University of Illinois Urbana-Champaign, Urbana, IL 61801; [c]National Center for Supercomputing Applications, University of Illinois Urbana-Champaign, Urbana, IL 61801; [d]Department of Natural Resources and Environmental Sciences, College of Agricultural, Consumer and Environmental Sciences, University of Illinois Urbana-Champaign, Urbana, IL 61801; [e]Climate and Global Dynamics Laboratory, The U.S. National Science Foundation National Center for Atmospheric Research, Boulder, CO 80305; [f]Department of Plant Biology, University of Illinois at Urbana-Champaign, Urbana, IL 61801; [g]Department of Biology and Graduate Degree Program in Ecology, Colorado State University, Fort Collins, CO 80523; [h]School of Geography, Development & Environment, University of Arizona, Tucson, AZ 85721; [i]Department of Agricultural and Consumer Economics, University of Illinois Urbana-Champaign, Champaign, IL 61801; [j]Department of Ecosystem Science and Sustainability, Colorado State University, Fort Collins, CO 80523; [k]Department of Biology, West Virginia University, Morgantown, WV 26506; [l]Department of Civil and Environmental Engineering, University of Illinois Urbana-Champaign, Urbana, IL 61801; [m]National Renewable Energy Laboratory, Golden, CO 80401; [n]Earth and Environmental Sciences Area, Lawrence Berkeley National Laboratory, Berkeley, CA 94720; and [o]The U.S. Department of Agriculture, Agricultural Research Service, Global Change and Photosynthesis Research Unit, Urbana, IL 61801

Author contributions: M.J., B.P., K.G., and M.K. designed research; M.J. and B.P. performed research; M.J. contributed new reagents/analytic tools; M.J., B.P., J.T., and P.M. analyzed data; M.J., B.P., K.G., D.M.L., E.H.D., A.K.K., G.A.B.-G., M.K., D.L.L., M.A.S., S.A.K., L.Z., J.M., J.T., C.J.B., P.M., F.M., D.L., and A.T. participated in discussion and provided feedback on the manuscript; and M.J., B.P., K.G., D.M.L., E.H.D., A.K.K., G.A.B.-G., M.K., D.L.L., M.A.S., S.A.K., L.Z., J.M., J.T., C.J.B., P.M., F.M., D.L., and A.T. wrote the paper.

1. J. K. Huang, C. Prayt, S. Rozelle, Enhancing the crops to feed the poor. *Nature* **418**, 678–684 (2002).
2. S. J. Davis *et al.*, Net-zero emissions energy systems. *Science* **360**, eaas9793 (2018).
3. C. Mora *et al.*, Broad threat to humanity from cumulative climate hazards intensified by greenhouse gas emissions. *Nat. Clim. Change* **8**, 1062–1071 (2018).
4. S. C. McClelland *et al.*, Managing for climate and production goals on croplands. *Nat. Clim. Change* **15**, 1–8 (2025).
5. N. S. Lewis, Research opportunities to advance solar energy utilization. *Science* **351**, aad1920 (2016).
6. S. Battersby, How to expand solar power without using precious land. *Proc. Natl. Acad. Sci. U.S.A.* **120**, e2301355120 (2023).
7. A. Goetzberger, Zastrow, On the coexistence of solar-energy conversion and plant cultivation. *Int. J. Solar Energy* **1**, 55–69 (1982).
8. C. Dupraz *et al.*, Combining solar photovoltaic panels and food crops for optimising land use: Towards new agrivoltaic schemes. *Renew. Energy* **36**, 2725–2732 (2011).
9. H. J. Williams, Y. Wang, B. Yuan, H. Wang, K. M. Zhang, Rethinking agrivoltaic incentive programs: A science-based approach to encourage practical design solutions. *Appl. Energy* **377**, 124272 (2025).
10. G. A. Barron-Gafford *et al.*, Agrivoltaics provide mutual benefits across the food–energy–water nexus in drylands. *Nat. Sustain.* **2**, 848–855 (2019).
11. J. T. Stid *et al.*, Impacts of agrisolar co-location on the food–energy–water nexus and economic security. *Nat. Sustain.* **8**, 1–12 (2025).
12. L. Kruitwagen *et al.*, A global inventory of photovoltaic solar energy generating units. *Nature* **598**, 604–610 (2021).
13. S. Wei, Y. Chen, Z. Zeng, An unexpectedly large proportion of photovoltaic facilities installed on cropland. *The Innovation Energy* **2**, 100070 (2025).
14. S. Amaducci, X. Yin, M. Colauzzi, Agrivoltaic systems to optimise land use for electric energy production. *Appl. Energy* **220**, 545–561 (2018).
15. N. Gomez-Casanovas *et al.*, Knowns, uncertainties, and challenges in agrivoltaics to sustainably intensify energy and food production. *Cell Rep. Phys. Sci.* **4**, 101470 (2023).
16. K. Knapp, M. A. Sturchio, Ecovoltaics in an increasingly water-limited world: An ecological perspective. *One Earth* **7**, 1705–1712 (2024).
17. M. A. Sturchio *et al.*, Grassland productivity responds unexpectedly to dynamic light and soil water environments induced by photovoltaic arrays. *Ecosphere* **13**, e4334 (2022).
18. C. S. Choi *et al.*, Environmental co-benefits of maintaining native vegetation with solar photovoltaic infrastructure. *Earth's Future* **11**, e2023EF003542 (2023).
19. S. A. Kannenberg, M. A. Sturchio, M. D. Venturas, A. K. Knapp, Grassland carbon–water cycling is minimally impacted by a photovoltaic array. *Commun. Earth Environ.* **4**, 238 (2023).
20. B. Valle *et al.*, Increasing the total productivity of a land by combining mobile photovoltaic panels and food crops. *Appl. Energy* **206**, 1495–1507 (2017).
21. S. Armstrong, J. Waldron, N. J. Whitaker, Ostle, Wind farm and solar park effects on plant–soil carbon cycling: Uncertain impacts of changes in ground-level microclimate. *Glob. Change Biol.* **20**, 1699–1706 (2014).
22. H. Marrou, L. Guilioni, L. Dufour, C. Dupraz, J. Wery, Microclimate under agrivoltaic systems: Is crop growth rate affected in the partial shade of solar panels? *Agric. For. Meteorol.* **177**, 117–132 (2013).
23. B. Zhang, R. Zhang, Y. Li, S. Wang, F. Xing, Ignoring the effects of photovoltaic array deployment on greenhouse gas emissions may lead to overestimation of the contribution of photovoltaic power generation to greenhouse gas reduction. *Environ. Sci. Technol.* **57**, 4241–4252 (2023).
24. H. Marrou, L. Dufour, J. Wery, How does a shelter of solar panels influence water flows in a soil–crop system? *Eur. J. Agron.* **50**, 38–51 (2013).
25. L. J. Walston *et al.*, Examining the potential for agricultural benefits from pollinator habitat at solar facilities in the United States. *Environ. Sci. Technol.* **52**, 7566–7576 (2018).
26. S. M. Grodsky, R. R. Hernandez, Reduced ecosystem services of desert plants from ground-mounted solar energy development. *Nat. Sustain.* **3**, 1036–1043 (2020).
27. V. Fthenakis, J. E. Mason, K. Zweibel, The technical, geographical, and economic feasibility for solar energy to supply the energy needs of the US. *Energy Policy* **37**, 387–399 (2009).
28. T. Feuerbacher, T. Herrmann, S. Neuenfeldt, M. Laub, A. Gocht, Estimating the economics and adoption potential of agrivoltaics in Germany using a farm-level bottom-up approach. *Renew. Sustain. Energy Rev.* **168**, 112784 (2022).
29. Food and Agriculture Organization of the United Nations (FAO), "FAO statistical databases" (2013). https://www.fao.org/faostat/. Accessed 19 June 2013.
30. C. Dupraz, Assessment of the ground coverage ratio of agrivoltaic systems as a proxy for potential crop productivity. *Agrofor. Syst.* **98**, 2679–2696 (2024).
31. J. F. von Liebig, *Die organische Chemie in ihrer Anwendung auf Agricultur und Physiologie* (Vieweg, 1840).
32. R. R. van der Ploeg, W. Böhm, M. B. Kirkham, On the origin of the theory of mineral nutrition of plants and the law of the minimum. *Soil Sci. Soc. Am. J.* **63**, 1055–1062 (1999).
33. Z. Xu, Y. Li, Y. Qin, E. Bach, A global assessment of the effects of solar farms on albedo, vegetation, and land surface temperature using remote sensing. *Solar Energy* **268**, 112198 (2024).
34. J. Ying, X. Gao, L. Yang, Z. Li, Y. Liu, Quantitative study of the environmental thermal effects of a photovoltaic power plant in the Gobi area-from the perspective of energy distribution. *Theor. Appl. Climatol.* **156**, 195 (2025).
35. E. Warmann, G. D. Jenerette, G. A. Barron-Gafford, Agrivoltaic system design tools for managing trade-offs between energy production, crop productivity and water consumption. *Environ. Res. Lett.* **19**, 034046 (2024).
36. A. Weselek *et al.*, Agrivoltaic system impacts on microclimate and yield of different crops within an organic crop rotation in a temperate climate. *Agron. Sustain. Dev.* **41**, 59 (2021).
37. S. Jiang *et al.*, Effects of different photovoltaic shading levels on kiwifruit growth, yield and water productivity under "agrivoltaic" system in Southwest China. *Agric. Water Manag.* **269**, 107675 (2022).
38. S. Poonia *et al.*, Techno-economic evaluation of different agri-voltaic designs for the hot arid ecosystem India. *Renew. Energy* **184**, 149–163 (2022).
39. A. Feuerbacher *et al.*, An analytical framework to estimate the economics and adoption potential of dual land-use systems: The case of agrivoltaics. *Agric. Syst.* **192**, 103193 (2021).
40. A. H. Schweiger, L. Pataczek, How to reconcile renewable energy and agricultural production in a drying world. *Plants People Planet* **5**, 650–661 (2023).
41. N. Zhang *et al.*, Booming solar energy is encroaching on cropland. *Nat. Geosci.* **16**, 932–934 (2023).
42. M. A. Sturchio *et al.*, Environmental controls of suppressed fall crop productivity in an agrivoltaic solar array. *Environ. Res. Food Syst.* **2**, 035004 (2025).
43. P. R. Malu, U. S. Sharma, J. M. Pearce, Agrivoltaic potential on grape farms in India. *Sustain. Energy Technol. Assess.* **23**, 104–110 (2017).
44. E. H. DeLucia *et al.*, Are we approaching a water ceiling to maize yields in the United States? *Ecosphere* **10**, e02773 (2019).

45. T. Partridge *et al.*, Irrigation benefits outweigh costs in more US croplands by mid-century. *Commun. Earth Environ.* **4**, 274 (2023).
46. L. Rosa *et al.*, Potential for sustainable irrigation expansion in a 3 °C warmer climate. *Proc. Natl. Acad. Sci. U.S.A.* **117**, 29526–29534 (2020).
47. Y. Li *et al.*, Climate model shows large-scale wind and solar farms in the Sahara increase rain and vegetation. *Science* **361**, 1019–1022 (2018).
48. A. Hu *et al.*, Impact of solar panels on global climate. *Nat. Clim. Change* **6**, 290–294 (2016).
49. R. K. Chopdar, N. Sengar, N. C. Giri, D. Halliday, Comprehensive review on agrivoltaics with technical, environmental and societal insights. *Renew. Sustain. Energy Rev.* **197**, 114416 (2024).
50. D. M. Lawrence *et al.*, The community land model version 5: Description of new features, benchmarking, and impact of forcing uncertainty. *J. Adv. Model. Earth Syst.* **11**, 4245–4287 (2019).
51. G. Danabasoglu *et al.*, The Community Earth System Model version 2 (CESM2). *J. Adv. Model. Earth Syst.* **12**, e2019MS001916 (2020).
52. C. J. Kucharik, Evaluation of a process-based agro-ecosystem model (Agro-IBIS) across the U.S. corn belt: Simulations of the interannual variability in maize yield. *Earth Interact.* **7**, 1–33 (2009).
53. S. Levis, A. Badger, B. Drewniak, C. Nevison, X. Ren, CLMcrop yields and water requirements: Avoided impacts by choosing RCP 4.5 over 8.5. *Clim. Change* **146**, 501–515 (2016).
54. G. D. Farquhar, S. von Caemmerer, J. A. Berry, A biochemical model of photosynthetic CO2 assimilation in leaves of C species. *Planta* **149**, 78–90 (1980).
55. D. L. Lombardozzi, G. B. Bonan, N. G. Smith, J. S. Dukes, R. A. Fisher, Temperature acclimation of photosynthesis and respiration: A key uncertainty in the carbon cycle-climate feedback. *Geophys. Res. Lett.* **42**, 8624–8631 (2015).
56. G. J. Collatz, M. Ribas-Carbo, J. A. Berry, Coupled photosynthesis-stomatal conductance model for leaves of C plants. *Aust. J. Plant Physiol.* **19**, 519–538 (1992).
57. B. E. Medlyn *et al.*, Reconciling the optimal and empirical approaches to modelling stomatal conductance. *Glob. Change Biol.* **17**, 2134–2144 (2011).
58. C. D. Koven *et al.*, The effect of vertically resolved soil biogeochemistry and alternate soil C and N models on C dynamics of CLM4. *Biogeosciences* **10**, 7109–7131 (2013).
59. J. D. Pelletier *et al.*, A gridded global data set of soil, intact regolith, and sedimentary deposit thicknesses for regional and global land surface modeling. *J. Adv. Model. Earth Syst.* **8**, 41–65 (2016).
60. D. L. Lombardozzi *et al.*, Simulating agriculture in the Community Land Model version 5. *J. Geophys. Res. Biogeosciences* **125**, e2019JG005529 (2020).
61. M. Jia *et al.*, Assessing the impact of agrivoltaics on water, energy, and carbon cycles using the Community Land Model version 5. *J. Adv. Model. Earth Syst.* 18, e2025MS005092 (2026).
62. Y. Elamri *et al.*, Rain concentration and sheltering effect of solar panels on cultivated plots. *Hydrol. Earth Syst. Sci.* **22**, 1285–1298 (2018).
63. A. M. Broadbent, E. S. Krayenhoff, M. Georgescu, D. J. Sailor, The observed effects of utility-scale photovoltaics on near-surface air temperature and energy balance. *J. Appl. Meteorol. Climatol.* **58**, 989–1006 (2019).
64. J. Zhang *et al.*, Model of evapotranspiration and groundwater level based on photovoltaic water pumping system. *Appl. Energy* **136**, 1132–1137 (2014).
65. J. Kim *et al.*, Shading impacts on sorghum and soybean grain yields in agrivoltaics systems: Source-sink strength in response to shading. *Smart Agricultural Technology* 12, 101647. (2025).
66. W. R. Wieder, J. Boehnert, G. B. Bonan, M. Langseth, "Regridded harmonized world soil database v1.2" (2014). https://www.earthdata.nasa.gov/data/catalog/ornl-cloud-hwsd-1247-1. Accessed 18 September 2014.
67. R. Cherian, J. Quaas, Trends in AOD, clouds, and cloud radiative effects in satellite data and CMIP5 and CMIP6 model simulations over aerosol source regions. *Geophys. Res. Lett.* **47**, e2020GL087132 (2020).
68. Q. E. Karhoff, A. B. Enders, J. L. Guarino, T. J. Swanson, Renewable energy in Illinois: The agrivoltaics contribution. *South. Illinois Univ. Law J.* **48**, 591 (2024).
69. J. P. Krasting *et al.*, NOAA-GFDL GFDL-ESM4 model output prepared for CMIP6 CMIP. *Earth System Grid Federation*, 10.26050/WDCC/AR6.C6CMNGGFEam (2018).
70. O. Boucher *et al.*, Presentation and evaluation of the IPSL-CM6A-LR climate model. *J. Adv. Model. Earth Syst.* **12**, e2019MS002010 (2020).
71. W. A. Müller *et al.*, A higher-resolution version of the Max Planck Institute Earth System Model (MPI-ESM1.2-HR). *J. Adv. Model. Earth Syst.* **10**, 1383–1413 (2018).
72. A. A. Sellar *et al.*, UKESM1: Description and evaluation of the UK Earth System Model. *J. Adv. Model. Earth Syst.* **11**, 4513–4558 (2019).
73. S. Yukimoto *et al.*, The meteorological research institute earth system model version 2.0, MRI-ESM2.0: Description and basic evaluation of the physical component. *J. Meteorol. Soc. Jpn. Ser.* **II**, 931–965 (2019).
74. B. Shipley, The AIC model selection method applied to path analytic models compared using ad-separation test. *Ecology* **94**, 560–564 (2013).
75. K. P. Burnham, D. R. Anderson, Eds.)., *Model Selection and Multimodel Inference: A Practical Information-Theoretic Approach* (Springer, New York, New York, NY, 2002).
76. J. S. Lefcheck, PiecewiseSEM: Piecewise structural equation modelling in R for ecology, evolution, and systematics. *Methods Ecol. Evol.* **7**, 573–579 (2016).
77. M. Jia, Agrivoltaics version of CLM5 (CLM5-AgPV) [Software]. *Figshare* (2025), 10.6084/m9.figshare.30122383.
78. M. Jia, Measurements for agrivoltaics sites. *Figshare* (2025), 10.6084/m9.figshare.28680176.v1.
79. C. Jiang, K. Guan, G. Wu, B. Peng, S. Wang, A daily, 250 m and real-time gross primary productivity product (2000–present) covering the contiguous United States. *Earth Syst. Sci. Data* **13**, 281–298 (2021).